JAST. Vol. 9, No. 2, pp 45-58

JAST Journal of Aerospace Science and Technology

The Utilization of High Fidelity Simulation in the Support of UAV Launch Phase Design: Three Case Studies

M. Mortazavi[1] , A. Askari[2]

Improvement of the launch phase of a jet powered Unmanned Aerial Vehicle (UAV) with Jet Assisted Take Off (JATO), has been the subject of attention in the UAV industry. Use of flight simulation tools reduces the risk and required some amount of flight testing for complex aerospace systems. In this research, full non-linear equations of motion are used to study and simulate this maneuver and three case studies of their application to UAV launch phase problems are presented. Attempt is also made to explain some aspects that were not definite in the test by simulation. The result of the examination is satisfactory. The second and third examples involve the flight test of the UAV. These two applications are typical of launch phase problems. The second example demonstrates a good applicability of this technique to improve and increase the stability of the UAV during launch. In the third example, the UAV in the presence of headwind shows that the simulation and real test have a good coincidence.

Nomenclauture

X_W, Y_W, Z_W	Aircraft location in inertial/world coordinates (m)	μ	Air viscosity
U_W, V_W, W_W	Aircraft velocity in inertial/world coordinates (m/sec)	$\delta_e, \delta_a, \delta_r$	Elevator, aileron and rudder deflection (rad)
Φ, θ, ψ	Azimuth, Elevation, Roll in inertial/world coordinates (radians)	S	Surface area of wing (m^2)
U, V, W	Linear velocity along X, Y and Z body axes (m/sec)	L, D, S_F	Lift, drag and side force
P, Q, R(or p, q, r)	Angular velocity around X, Y and Z body axes (rad/sec)	b	Wing span (m)
V_τ	Resultant velocity vector ($\sqrt{U^2+V^2+W^2}$)	C	Chord length (m)
$V_{\tau\ Stall}$	Stall speed (m/sec)	l_f	UAV length
RE_V	Reynolds number at V_τ	D_f	UAV fuselage section diameter
RE_{Stall}	Reynolds number at $V_{\tau\ Stall}$	X_{cgV}	Longitudinal distance of variable cg position from nose of the UAV
V_ε	Wind velocity across tail of aircraft	Z_{cgV}	Vertical distance of variable cg position from the lowest point of fuselage of the UAV
$\dot{U},\dot{V},\dot{W}$	Linear acceleration (m/sec^2)	X_{pin}	Longitudinal distance of pin position from nose of the UAV
$\dot{P},\dot{Q},\dot{R}$	Angular acceleration (rad/sec^2)	Z_{pin}	Vertical distance of pin position from the lowest point of fuselage of the UAV
F_x, F_y, F_z	Forces acting on aircraft in body axes	W	Weight (N)
l, m, n	Moments about the X, Y and Z axes	M_{UAV}	Mass of the UAV
a	Angle of attack [$\tan^{-1}$(W/U)]	M_{JATO}	Mass of JATO
b	Sideslip [$\tan^{-1}$(V/U)]	$M_{JATO\,Case}$	Mass of JATO without propellant
ρ	Air density	$X_{JATO\ nose}$	Longitudinal distance of nose of JATO from nose of the UAV
		$Z_{JATO\ nose}$	Vertical distance of nose of JATO from the lowest point of fuselage of the UAV
		α_{JATO}	Angle between JATO and UAV longitudinal axis in XZ-plane
		α_{MJT}	Angle between JATO and UAV longitudinal axis in XY-plane
		I_{xx}, I_{yy}, I_{zz}	Moment of inertia (kg-m2)
		Subscript 'W'	Inertial/World coordinate system

1. Associate professor, Aerospace Engineering Department, Amirkabir University of Technology, Tehran, Iran, E-mail address: mortazavi@aut.ac.ir

2. PhD candidate, Aerospace Engineering Department, Amirkabir University of Technology, Tehran, Iran, E-mail address: askari@aut.ac.ir

Longitudinal Coefficients

C_{L0}	Reference lift at zero angle of attack
C_{D0}	Reference drag at zero angle of attack
$C_{L\alpha}$	Lift curve slope
$C_{D\alpha}$	Drag curve slope
C_{m0}	Pitching moment at zero angle of attack
$C_{m\alpha}$	Pitching moment due to angle of attack
C_{Lq}:	Lift due to pitch rate
C_{mq}	Pitch moment due to pitch rate
$C_{L\dot{\alpha}}$	Lift due to angle of attack rate
$C_{m\dot{\alpha}}$	Pitch moment due to angle of attack rate

Lateral Coefficients

$C_{Y\beta}$	Side force due to sideslip
$C_{l\beta}$	Dihedral effect
C_{lP}	Roll damping
C_{lR}	Roll due to yaw rate
$C_{n\beta}$	Weather cocking stability
C_{nP}	Rudder adverse yaw
C_{nR}:	Yaw damping

Control Coefficients

$C_{L\,\delta e}$	Lift due to elevator
$C_{D\,\delta e}$	Drag due to elevator
$C_{m\,\delta e}$	Pitch due to elevator
$C_{l\,\delta a}$	Roll due to aileron

1 Introduction

Today, there is considerable interest in Unmanned Aerial Vehicle (UAV) which is characterized by jet engine, zero length launcher and launching with JATO[1].

The quality of launch will have a significant effect on the overall UAV performance and safety of flight. The best available synthesis and analysis techniques should, therefore, be used. The use of the simulation ultimately had a significant impact on the safety and the cost-effectiveness of exploring this high risk portion of the flight test program.

Simulation analysis also proved valuable in developing and assessing the successful modification of the launch phase.

Recent developments in the practical application of simulation theory combined with the availability of computer-based synthesis and analysis tools offer the potential for significant improvements in flight quality during launch and also in reduction of the associated development flight test cost.

The use of airplane simulation has an extensive history. Mathematical models used to describe these configurations were very simple, derivative-based, usually hand-adjusted by engineers and guided by pilots' subjective inputs as well as flight test result. As the expense of flight test has increased proportionally with the cost of airplanes and the introduction of automatic flight controls, the need and importance of developing high fidelity simulations prior to flight has also increased. Successful utilization of simulation in the launch phase, typified by non-linear and non-symmetric aerodynamic characteristics, would significantly enhance the safety of the flight test program.

There have been many attempts to generate and improve modeling of the airplane's dynamic model, which ultimately improve the simulation's predictive capabilities for flight test [2,3,4,5,6].

Here, the implementation of launch phase simulation for a specific UAV is described. Some launch tests are performed. The purpose of the test programs is to validate the system design and the simulation algorithm.

UAV launch phase is one of the most important critical phases of a UAV and many failures occur in this phase. Some reasons are: 1. System instability in the launch phase, 2. The complexity of the aerodynamic behavior (the system flies in the range of a very low Reynolds number to a high Reynolds number) and 3. Occurrence of phenomena such as "Misalignment of JATO Thrust" or "Unsimultaneous Cut of Pins". Because of these reasons, it is not possible to use a simple simulation for the UAV launch phase. Therefore, the objective of this paper is to develop the launch phase simulation of the UAVs. This is the first contribution of this paper.

There are some papers on the subject of UAVs launch phase simulation. However, it should be noted that the launch phase simulation of a UAV with this level of details such as "Misalignment of JATO Thrust" or "Unsimultaneous Cut of Pins" is introduced for the first time in the UAV launch phase simulation in the present article. Therefore, the approach of launch phase simulation, in this article is unique and there is no similar work in the other studies. More importantly, it should be noted that three real case studies shows the simulation can accurately predict the system behavior in the launch phase. Actually, this simulation would be very beneficial to predict the future behavior of the system in the various flight conditions or in the presence of disturbances such as gust and turbulence. Hence, this article discusses the issues that are important in the launch phase of the UAVs which have not been addressed pre-

viously. This is the second contribution of this paper.

This article is also provided as an educational issue for the flight mechanics engineers who are working on the subject of the UAV launch phase simulation. First, the considerations that should be taken into account in the UAV launch phase have been studied. Then, the test results are presented to achieve two goals: 1. verifying the simulation, 2. finding the differences between the simulation and test results and also providing a stepwise logical analysis to explain these differences. Therefore, the focal point of this paper is to propose a high fidelity simulation in order to predict the safety factor of the UAV launch phase.

Flight Dynamic Modeling

Coordinate System and Terminology

In airplane simulations, coordinate systems fall into two broad classes, body coordinates and inertial or world coordinates [3,5]. All aerodynamic forces, accelerations and velocities are calculated in the body coordinate system and then converted to the inertial or world coordinate system prior to updating an airplane's position and attitude.

Figure 1 shows the generally accepted convention for labeling the axes in the two coordinate systems. Body coordinates are defined with the origin at the center of gravity and inertial or world coordinates are defined with the origin based at a fixed point on the ground. Because of its limited effect, the curvature of the earth is ignored [4,5]. Most terms described in this paper refer to the geometric body axes. However, if a reference is made to the inertial or world coordinate system the subscript 'w' is used (Figure 1).

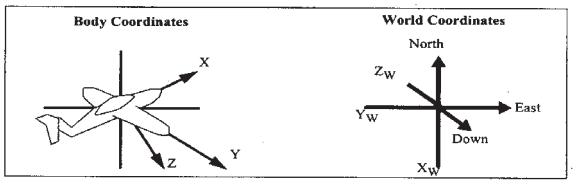

Figure 1. body coordinate and inertial/world systems

The mathematical model presented takes forces, control inputs and aircraft specifications as inputs, while generating linear and angular velocities in aircraft body coordinates as outputs (Figure 2).

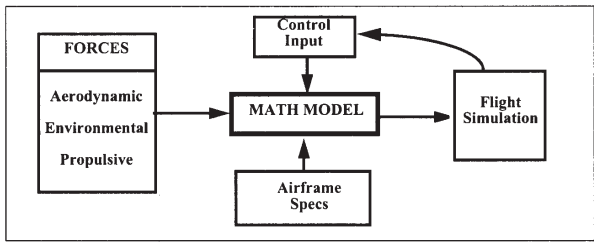

Figure 2. Mathematical Model

The flat-earth body axes 6-DOF equations of motion of an airplane are [2,5]:

Force equations:

$$\dot{U} = VR - WQ - g\sin\theta + F_X/m \tag{1}$$

$$\dot{V} = WP - UR + g\sin\phi\cos\theta + F_Y/m \tag{2}$$

$$\dot{W} = UQ - VP + g\cos\phi\cos\theta + F_Z/m \tag{3}$$

Moment equations:

$$I_{XX}\dot{P} - I_{XZ}\dot{R} - I_{XZ}PQ + (I_{ZZ} - I_{YY})RQ = l \tag{4}$$

$$I_{YY}\dot{Q} + (I_{XX} - I_{ZZ})PR + I_{XZ}(P^2 - R^2) = m \tag{5}$$

$$I_{ZZ}\dot{R} - I_{XZ}\dot{P} + (I_{YY} - I_{XX})PQ + I_{XZ}RQ = n \tag{6}$$

Kinematic equations:

$$P = \dot{\phi} - \dot{\psi}\sin\theta \tag{7}$$

$$Q = \dot{\theta}\cos\phi + \dot{\psi}\sin\phi\cos\theta \tag{8}$$

$$R = -\dot{\theta}\sin\phi + \dot{\psi}\cos\phi\cos\theta \tag{9}$$

Navigation equations:

$$\begin{bmatrix}\dot{X}_W\\ \dot{Y}_W\\ \dot{h}_W\end{bmatrix} = \begin{bmatrix}\cos\psi & -\sin\psi & 0\\ \sin\psi & \cos\psi & 0\\ 0 & 0 & 1\end{bmatrix}.$$

$$\begin{bmatrix}\cos\theta & 0 & \sin\theta\\ 0 & 1 & 0\\ -\sin\theta & 0 & \cos\theta\end{bmatrix}\begin{bmatrix}1 & 0 & 0\\ 0 & \cos\phi & -\sin\phi\\ 0 & \sin\phi & \cos\phi\end{bmatrix}\begin{bmatrix}U\\ V\\ W\end{bmatrix}$$

The forces and moments are:

$$F_X = F_{X\,A} + F_{engine} + F_{X\,JATO} \quad (11)$$

$$F_Y = F_{Y\,A} + F_{Y\,JATO} \quad (12)$$

$$F_Z = F_{Z\,A} + F_{Z\,JATO} \quad (13)$$

$$l = l_A + l_{JATO} \quad (14)$$

$$m = m_A + m_{engine} + m_{JATO} \quad (15)$$

$$n = n_A + n_{JATO} \quad (16)$$

Engine forces, torque and gyroscopic effect as well as environmental forces such as wind shear can have anywhere from a minor to significant effect on the forces and moments along all axes of the aircraft [3]. In order to limit this complexity of the model, some simplifications are made. Engine thrust is limited to the X-axis located above the aircraft center line that makes m_{Thrust} and no calculations are made for the gyroscopic effect of a jet engine [3,5].

Aerodynamic Model

The terms F_{AX}, F_{AY} and F_{AZ} represent the resultant aerodynamic forces.

$$F_{X\,A} = -L\sin\alpha - D\cos\alpha - S_F\sin\beta \quad (17)$$

$$F_{Y\,A} = S_F\cos\beta \quad (18)$$

$$F_{Z\,A} = -L\cos\alpha - D\sin\alpha \quad (19)$$

Using the non-dimensional coefficients, lift, drag and sideforce are calculated as follows:

$$L = \left[\begin{array}{l} C_{L0} + C_{L_\alpha}\alpha + C_{Lq}q\dfrac{c}{2V_\tau} + \\ C_{L_{\dot\alpha}}\dot\alpha\dfrac{c}{2V_\tau} + C_{L_{\delta e}}\left[\dfrac{V_\tau + \Delta V_\varepsilon}{V_\tau}\right]^2 \end{array}\right]\bar{q}S \quad (20)$$

$$D = \left[\begin{array}{l} C_{D0} + C_{D_\alpha}\alpha + C_{Dq}q\dfrac{c}{2V_\tau} + \\ C_{D_{\dot\alpha}}\dot\alpha\dfrac{c}{2V_\tau} + C_{D_{\delta e}}\left[\dfrac{V_\tau + \Delta V_\varepsilon}{V_\tau}\right]^2 \end{array}\right]\bar{q}S \quad (21)$$

$$S_F = (C_{Y_\beta} + C_{Y_{\delta r}}\delta r)\bar{q}S \quad (22)$$

The aerodynamic moments represent the torque about the center of mass of the aircraft and are determined in the following equations:

$$l_A = \left[\begin{array}{l} C_{l_\beta}\beta + C_{l_P}P\dfrac{b}{2V_\tau} + \\ C_{l_R}R\dfrac{b}{2V_\tau} + C_{l_{\delta a}}\delta a + C_{l_{\delta r}}\delta r \end{array}\right]\bar{q}Sb \quad (24)$$

$$m_A = \left[\begin{array}{l} C_{mo} + C_{m_\alpha}\alpha + C_{mq}q\dfrac{c}{2V_\tau} + \\ C_{m_{\dot\alpha}}\dot\alpha\dfrac{c}{2V_\tau} + C_{m_{\delta e}}\left[\dfrac{V_\tau + \Delta V_\varepsilon}{V_\tau}\right]^2 \end{array}\right]\bar{q}Sc \quad (25)$$

$$n_A = \left[\begin{array}{l} C_{n_\beta}\beta + C_{n_P}P\dfrac{b}{2V_\tau} + \\ C_{n_R}R\dfrac{b}{2V_\tau} + C_{n_{\delta a}}\delta a + C_{n_{\delta r}}\delta r \end{array}\right]\bar{q}Sb \quad (26)$$

UAV Characteristics

The UAV characteristics are shown in table 1 [8].

Item	Nomenclature	Quantity
1	External Dimensions	
1.1	Wing Span	3 m
1.2	Wing Aspect Ratio	4
1.3	Mean Aerodynamic Chord	0.8 m
1.4	Fuselage Length	5.5 m
1.5	Fuselage Diameter	0.42 m
1.6	Wing Area	2.25 m^2
1.7	C.G. Position From Nose	3.13 m
2	Weight	
2.1	Gross Weight	425 kg
2.2	Launch Weight	475 kg
3	Aerodynamic	
3.1	Wing Lift Curve Slope	0.068 /rad
3.2	Zero Lift Coefficient	0.15
3.3	Horizontal L.C.S.	0.062 /rad
3.4	Vertical L.C.S	0.062 /rad
4	Performance	
4.1	ISA Condition	
4.2	Stall Speed	70 m/s
4.3	Engine Thrust	3500 N

Table 1- UAV general characteristics

Aerodynamic Forces and Moments Correction

The idea used in this research for the aerodynamic forces and moments in low a Reynolds number, is to consider a linear and quadratic relation between Reynolds and Aerodynamic forces and moments as below:

$$RE_V = \rho V_\tau l_f / \mu, \quad RE_{Stall} = \rho V_{\tau\ Stall} l_f / \mu \tag{27}$$

$$for \quad RE_V < RE_{Stall}:$$

$$\left(F_{X,Y,Z}, M_{X,Y,Z}\right) = \frac{RE_V}{RE_{Stall}}\left(F_{X,Y,Z}, M_{X,Y,Z}\right) \tag{28}$$

$$\left(F_{X,Y,Z}, M_{X,Y,Z}\right) = \left(\frac{RE_V}{RE_{Stall}}\right)^2 \left(F_{X,Y,Z}, M_{X,Y,Z}\right) \tag{29}$$

where $F_{X,Y,Z}$ and $M_{X,Y,Z}$ are the forces and moments in equations 11 to 16.

JATO Model

Figure 3 shows the ideal JATO thrust model. JATO thrust is as follows:

$$F_{X\,JATO} = T_{JATO}\cos(\alpha_{JATO}) \tag{30}$$

$$F_{Y\,JATO} = 0 \tag{31}$$

$$F_{Z\,JATO} = T_{JATO}\sin(\alpha_{JATO}) \tag{32}$$

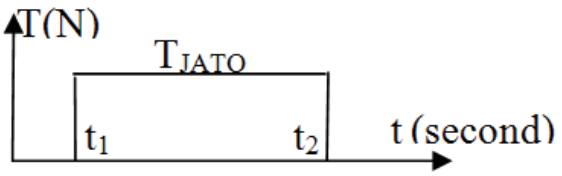

Figure 3. JATO thrust model

JATO Installation on the UAV

Figure 4 shows the schematic installation of the JATO under the UAV. Increasing α_{JATO}, causes an instability behavior and decreasing it, causes the UAV not to reach a proper altitude. Obviously, the JATO thrust line must pass through the $cg_{(UAV+JATO)}$.

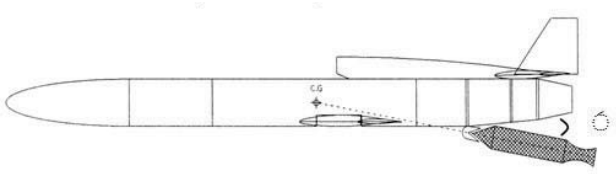

Figure 4. JATO location on the UAV

Misalignment of JATO Thrust

Ideally, there is no misalignment in JATO thrust, but actually JATO thrust line is not on the JATO longitudinal axis.

Asymmetric Forces and moments acting on the UAV when JATO thrust is aligned to right side are:

(MJT: Misalignment of JATO Thrust)

$$T_{Long.\,JATO} = T_{JATO}\cos(\alpha_{MJT}) \tag{33}$$

$$T_{Lateral\ JATO} = T_{JATO}\sin(\alpha_{MJT}) \tag{34}$$

$$F_{X\ MJT} = T_{Long.\ JATO}\cos(\alpha_{JATO}) \tag{35}$$

$$F_{Y\ MJT} = T_{Lateral\ JATO} \tag{36}$$

$$F_{Z\ MJT} = T_{Long.\ JATO}\sin(\alpha_{JATO}) \tag{37}$$

$$m_{MJT} = F_{X\ MJT}(X_{cg\,V} - X_{JATO\ nose}) + F_{Z\ MJT}(Z_{cg\,V} - Z_{JATO\ nose}) \tag{38}$$

$$n_{MJT} = F_{Y\ MJT}(X_{cg\,V} - X_{JATO\ nose}) \tag{39}$$

$$l_{MJT} = -F_{Y\ MJT}(Z_{cg\,V} - Z_{JATO\ nose}) \tag{40}$$

Unsimultaneous Cut of Pins

The UAV is connected to the launcher by two pins (figure 5). When JATO thrust reaches 70%, the pins cut and the UAV separates from the launcher. It is necessary to check the UAV behavior when pins do not cut simultaneously.

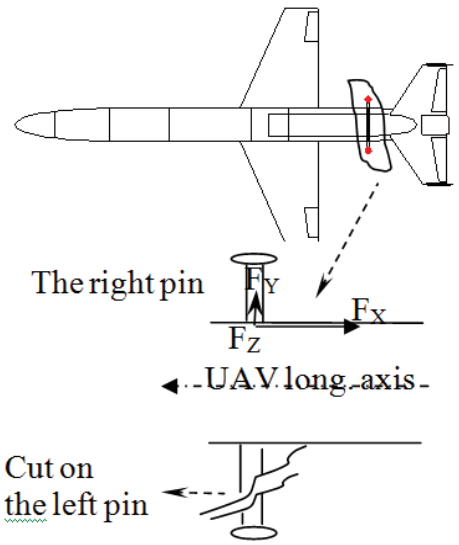

Figure 5. UAV connection to launcher (F_z is perpendicular and toward the page)

Where the left pin cut, forces and moments acting on the UAV are:

(UCP: Unsimultaneous Cut of Pins)

$$F_{X\,UCP} = -F_{X\,MJT} - F_{engine} \tag{41}$$

$$F_{Y\,UCP} = -F_{Y\,MJT} \tag{42}$$

$$F_{Z\,UCP} = -F_{Z\,MJT} \tag{43}$$

$$m_{UCP} = -F_{X\,UCP}(Z_{cg\,V} - Z_{pin}) + \\ - F_{Z\,UCP}(X_{cg\,V} - X_{pin}) \tag{44}$$

$$n_{UCP} = F_{X\,UCP}(d_f/2) + F_{Y\,UCP}(X_{cg\,V} - X_{pin}) \tag{45}$$

$$l_{UCP} = F_{Z\,UCP}(d_f/2) + F_{Y\,UCP}(Z_{cg\,V} - Z_{pin}) \tag{46}$$

Total JATO forces and moments acting on the UAV are

$$F_{X\,JATO} = F_{X\,MJT} + F_{X\,UCP} \tag{47}$$

$$F_{Y\,JATO} = F_{Y\,MJT} + F_{Y\,UCP} \tag{48}$$

$$F_{Z\,JATO} = F_{Z\,MJT} + F_{Z\,UCP} \tag{49}$$

$$m_{JATO} = m_{MJT} + m_{UCP} \tag{50}$$

$$n_{JATO} = n_{MJT} + n_{UCP} \tag{51}$$

$$l_{JATO} = l_{MJT} + l_{UCP} \tag{52}$$

Center of Gravity and Moment of Inertia

At first, the dynamic system is UAV and JATO, after that JATO fuel is finished and the case of the JATO is separated from UAV. The variable cg position is:

t_1<Time<t_2:

$$\vec{r}_{g\,Var} = \frac{M_{UAV}\,\vec{r}_{g\,UAV} + M_{JATO}\,\vec{r}_{g\,JATO}}{M_{UAV} + M_{JATO}} \tag{53}$$

Time=t_2:

$$\vec{r}_{cg_{Var}} = \frac{M_{UAV}\,\vec{r}_{cg_{UAV}} + M_{JATOCase}\,\vec{r}_{cg_{JATOCase}}}{M_{UAV} + M_{JATOCase}} \tag{54}$$

Time>t_2 :

$$\vec{r}_{g\,Var} = \vec{r}_{g\,UAV} \tag{55}$$

Change of weight and moment of inertia of the system (UAV+JATO) during JATO burning are considered in the simulation.

Correction of the UAV Coefficients

Because of changing the cg location, the correction on the moment coefficients is:

$$C_{m\,(UAV+JATO)} = C_{m\,UAV} + \\ + C_{L\,UAV}[(\bar{X}_{cg\,(UAV+JATO)} - \bar{X}_{cg\,UAV}) - \bar{X}_{ac}] \tag{56}$$

At first, time<t_1 and cg position move back, causing a decrease in the stability margin that must be considered in the analysis.

Definition of the Problem

The simulation model should predict the UAV attitude, position and velocity in launch phase before the test. The simulation results are compared with three launch/flight test results. After verifying the software, sensitivity analysis using simulation can be helpful to increase the insight of parameter effectiveness in the launch phase.

Results and Discussions

Case Studies

Three case studies of launch simulation of the UAV are presented. All of the case studies involve two control surfaces: δ_e, δ_a that may be changed by operator and/or pitch/roll attitude hold/select mode control. The first test launch is without engine and the second and third tests are launched with engine.

Measurement devices are vertical gyro, GPS receiver, barometric altimeter and telecommunication apparatus. All these devices were calibrated and have been used before on the other UAVs. Measurement parameters are pitch angle, bank angle, altitude, pressure altitude, temperature, latitude, longitude, and ground speed. Note that the frequency of flight test data recording is 1 HZ. This fact causes some data loss and decreases the precision of the test data in comparison with the simulation result. Because of this, the simulation and test results can be compared in large scale.

Case Study I: Launch Test without Engine

The UAV weight is 420 kg and JATO produces 24 KN in average during t_2-t_1=2.2 seconds. The simulations and the flight test in the case study I, are in the same condition: $\alpha_{JATO}=10.67^0$, $\theta_0=20^0$, temp=ISA+10, $\delta_e=5^0$,$t_1=0$.

To show the correction factor which is considered in equations 27 and 29, four scenarios are considered as below:

Scenario 1: simulation of the launch phase considering the quadratic correction factor $(RE_V/RE_{Stall})^2$ in equation 29.

Scenario 2: simulation of the launch phase considering the linear correction factor (RE_V/RE_{Stall}) in equation 28.

Scenario 3: simulation of the launch phase without considering correction factor (RE_V/RE_{Stall}) in equation 28.

Scenario 4: simulation of the launch phase considering zero forces and moments for $RE_V < RE_{Stall}$.

Simulation of scenario 1 and 2 are shown in figure 6. There is a good agreement in altitude between scenario 1 and the flight test. There are about 5 percent errors in altitude between scenario 1 and the flight test and about 13 percent error between scenario 2 and the flight test. Therefore, it can be concluded that considering the quadratic form of the correction factor for forces and moments (equation 29) is more accurate than the linear model (equation 28). Figure 7 shows simulation of scenario 3 and 4. Scenario 3 is not acceptable, because pitch angle and altitude are not in their reasonable range. Although scenario 4 looks acceptable, there is an error of about 25 percent in altitude between this scenario and the flight test.

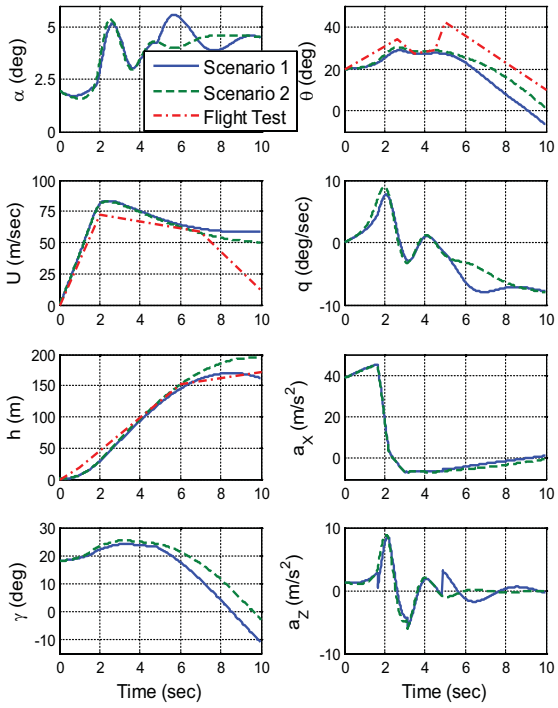

Figure 6. Simulation of the UAV – Scenario 1,2

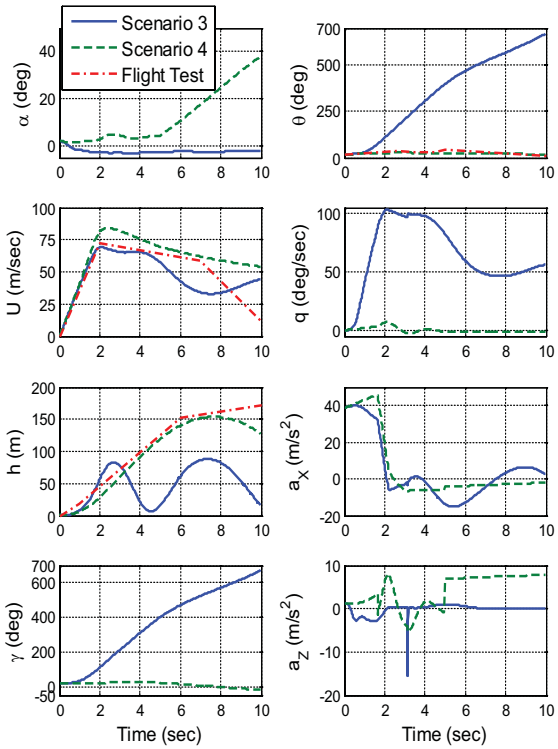

Figure 7. Simulation of the UAV – Scenario 3,4

Figure 8 shows simulation and flight test of the UAV. There is about 5 percent error in altitude and 6 percent error in velocity that shows a good agreement. Differences in speed after t=7 seconds can be because of some problems in the manufacturing of the first prototype. Therefore, the drag coefficient in the real model is larger than is the one considered in the simulation. Another effect is because of lateral oscillation that causes loss of UAV energy and reduces speed to lower than the point predicted in the simulation.

Pitch angle and bank angle in figure 8 are different in simulation and test. It seems a pilot command after t=4 seconds in δ_E. Simulation verifies this idea (figure 10). Also, during JATO burning, the bank angle increases to 30^0. Using simulation, it is concluded that this occurs because of both JATO misalignment in xy-plane and non-simultaneous cut of pins ($\alpha_{MJT}=0.01^0$, $\Delta t_{UCP}=0.01$ sec).

Although speculating what the pilot may have thought is difficult, two kinds of scenarios are assumed. Figure 9 illustrates simulation of the test using an unstable autopilot during 10 seconds–maximum altitude time. The gain of bank attitude hold mode is deliberately selected as $K_\varphi=12$ and $\varphi_{Comm.}=0^0$. Figure 9 does not resemble what happened in the real test. The bank angle gradually increases during 10 seconds and the maximum amplitude is about 25^0;two points which are different from the test. Another assumption is the pilot's reaction to hold the bank angle near zero. Figure 10 illustrates simulation of the UAV with pilot in the loop. The figure shows a similarity between the simulation and the test. Therefore, it is concluded that the pilot tried to stabilize the UAV in longitudinal and lateral-directional modes.

As a result, because the UAV has a high acceleration during launch, pilot commands cause an instability behavior and the suggestion is using the flight control system. Figure 11 shows the UAV can be effectively controled with a stable gain autopilot which is shown in figure 12 ($K_\varphi=0.5$).

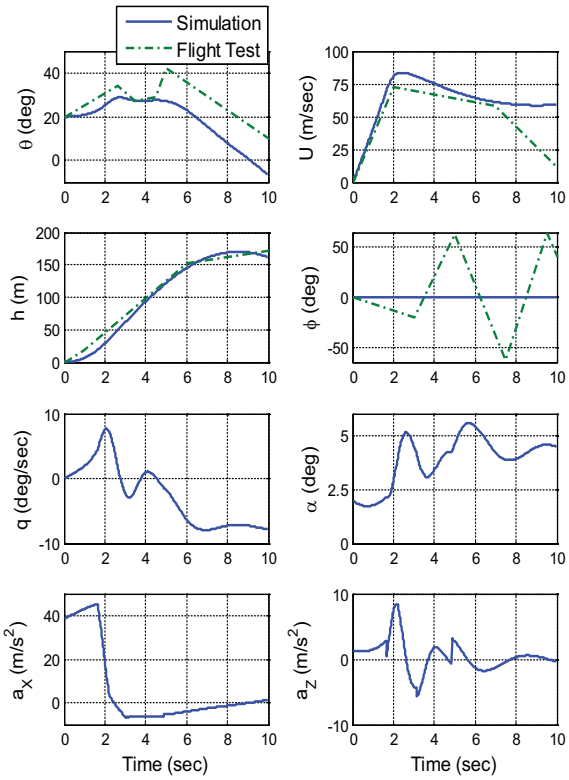

Figure 8. Simulation and flight test of the UAV

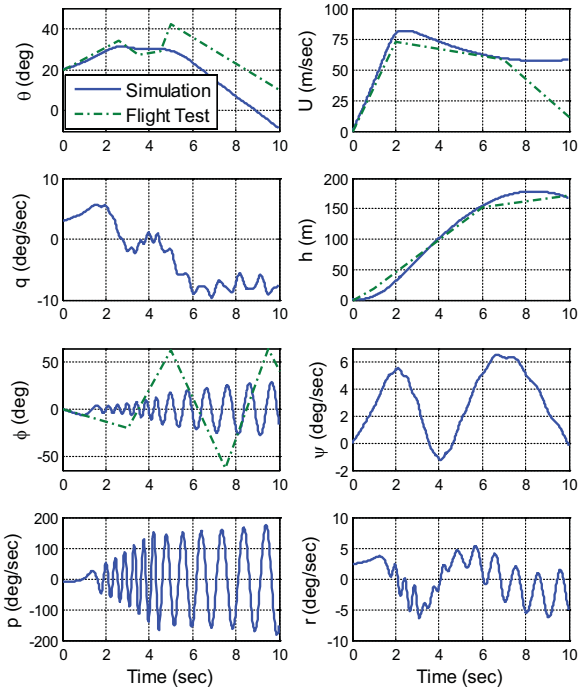

Figure 9. Simulation of the UAV
Using autopilot command with an unstable gain ($K_\varphi=2.2$)

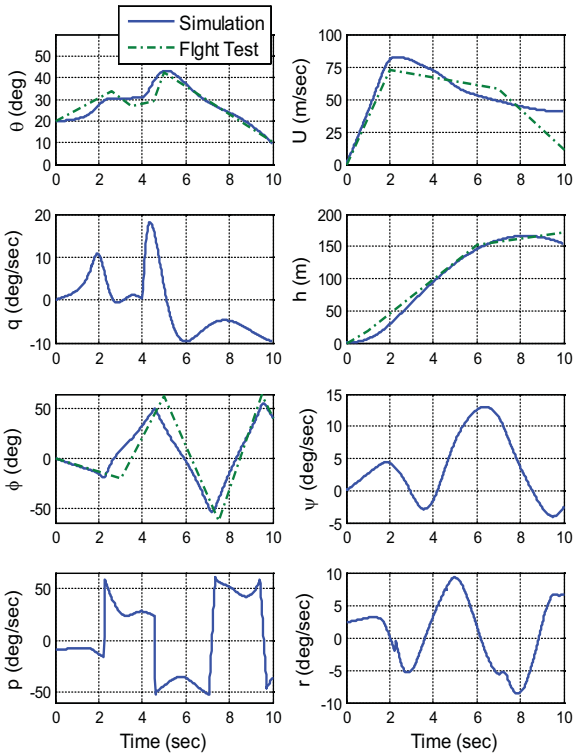

Figure 10. Simulation of the UAV Using operator command

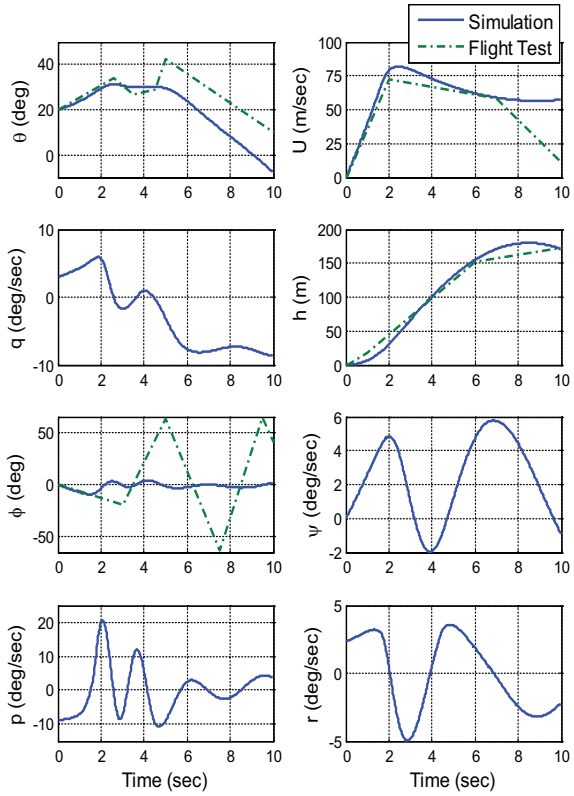

Figure 11. Simulation of the UAV Using autopilot command with a stable gain (K_φ=0.2)

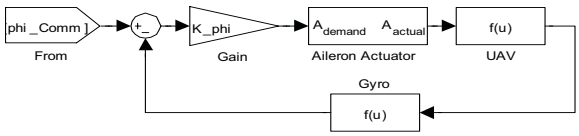

Figure 12. Roll Attitude Hold/Select Mode autopilot

Case Study II: Launch Test with Engine

In this test, the prototype has an engine that produces a thrust of about 3 KN. The UAV weight is 280 kg; which is the empty weight. The JATO thrust is 11700 N during t_2-t_1=2.12 seconds. Simulation and flight test in the case study II, are in the same condition: $\alpha_{JATO}=15.5^0$, $\theta_0=20^0$, temp=ISA+10, $\delta_{e\,0}=10^0$,t_1=0.

Figure 13 illustrates the simulation and flight test of the UAV. Lateral-directional parameters are near zero and ignorable. The difference between t_2 in simulation and test is due to the difference in the burning time of the JATO ideal and actual models used for simulation and test, respectively. The difference between t_2 in the simulation and the test is due to difference in the burning time of JATO considered in ideal and actual models for simulation and test, respectively. Like case study I, due to pilot command during t=2 and t=4 seconds, cause pitch angle is lower than that in the simulation. Therefore, velocity in the simulation is lower than the test. From the figure, altitude error is about 7 percent which is acceptable.

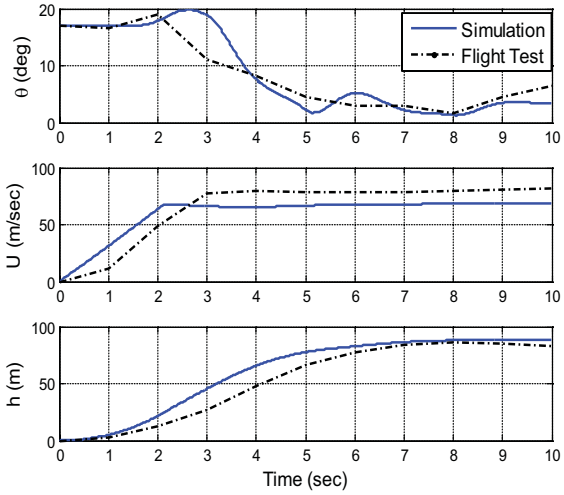

Figure 13. Simulation of the UAV

Case Study III: Launch Test in The Presence of Headwind

The UAV weight is 420 kg and JATO averagely produces 24 KN during t_2-t_1=2.2 sec. In the test, there is a headwind equal to 30 km/h. The purpose is to control the UAV in the presence of headwind. The simulation and flight test in the case study III are in the same condition: $\alpha_{JATO}=11.6^0$, $\theta_0=20^0$, temp=ISA+10, $\delta_{e\,0}=10^0$, $t_1=0$.

Figure 14 illustrates flight test and simulation of the UAV. Because of headwind, the pitch angle increases about 12^0 in second times. From the figure, there is a good agreement of the pitch angle in the simulation and the test. After t=3 seconds, a pitch autopilot tries to keep the pitch angle equal to $\theta_{Command}=15^0$.

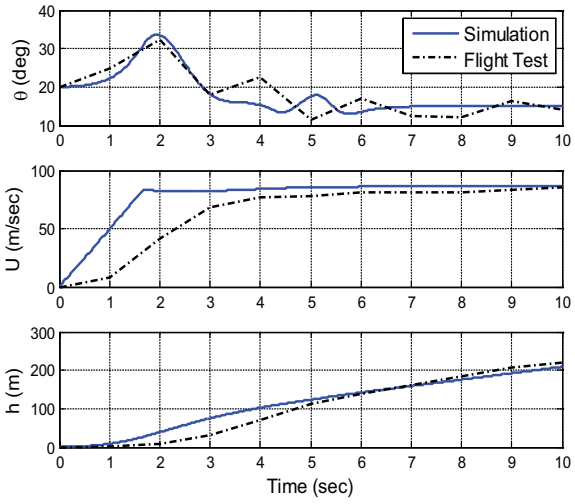

Figure 14. Simulation and flight test of the UAV in the presence of headwind=30 km/h

As discussed in case study II, because the impulses in JATO ideal and actual models are equal and burning times are different, as can be seen in the figure 14, the velocity and altitude are different at first, but they become equal after 10 seconds.

In this test, by removing some problems existing in the last two tests like pilot command or an accurate prototype, there are no differences between simulation and test after 10 seconds.

Sensitivity Analysis

Three case studies show there is a high fidelity simulation and, therefore, it is possible to use this simulation as a design tool and in sensitivity analysis in order to measure the sensitivity of the UAV variables to parameter variation in the launch phase. Actually, it helps designing the launch parameters such as α_{JATO}, θ_0, JATO thrust and duration (T_{JATO}, t_{JATO}), maximum Δt_{UCP} and maximum α_{MJT}. Thus it could decrease the flight test cost.

Table 2 includes different JATOs with similar impulses, different launch angles (θ_0), JATO angles (α_0), JATO misalignment and non-simultaneous cuts of pins. The initial data is: $T_{JATO}=25$ KN, $t_2=2.2$ sec, $\theta_0=20^0$, $\alpha_0=10^0$, $\delta_{e0}=5^0$ [7].

Case	T_{JATO} KN	t_{JATO} sec	Imp. KN.s	θ_0 deg	α_{JATO} deg	$\Delta\alpha_{JATO}$ deg	Δt_{Pins} sec
1	55, 25, 13.7	1, 2.2, 4	55	20^0	10^0	0	0
2	25	2.2	55	10^0, 20^0, 40^0	10^0	0	0
3	25	2.2	55	15^0	5^0, 10^0, 20^0	0	0
4	25	2.2	55	20^0	10^0	.001, .01, .1	0
5	25	2.2	55	20^0	10^0	0	.001, .01, .1

Table 2. Case studies for the launch - $\delta_{e0}=5^0$

The case studies of launch phase simulation of different parameters are specified in figures 15 to 22. Figure 15 introduces three JATO models with the same impulse used for launch. Figure 16 shows using JATO with $T_{JATO}=50$ KN decreases the stability and JATO with $T_{JATO}=13.75$ KN, decreases the altitude (figure 16). An increase in the launch angle (θ_0) causes decrease in the velocity that may be lower than the stall speed. Conversely, decreasing it causes a decrease in the altitude, as can be seen in figure 17. Figure 18 shows high α_{JATO} decreases the angle of attack during the first two seconds and the stability of the UAV. On the contrary, low α_{JATO} decreases altitude, which is not enough for recovery in emergency conditions. Trend study in figures 19 and 20 illustrate the maximum time difference between pin cuts must not exceed 0.05 sec ($\Delta t_{Pins}\leq 0.05$ sec). If $\Delta t_{Pins}>0.05$ sec, the UAV might be unstable in both longitudinal and lateral-directional modes. Similarly, based on figures 21 and 22, the maximum JATO misalignment must not exceed 0.05^0 ($\Delta\alpha_{Unsymmetric}\leq 0.05^0$), otherwise there would be instability in the lateral-directional mode.

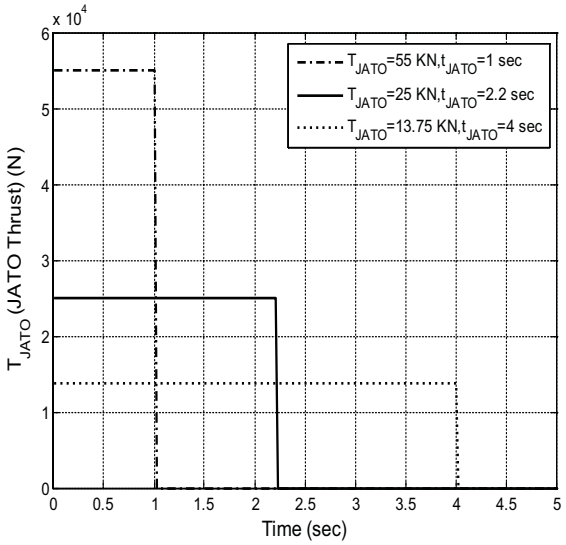

Figure 15. Case 1

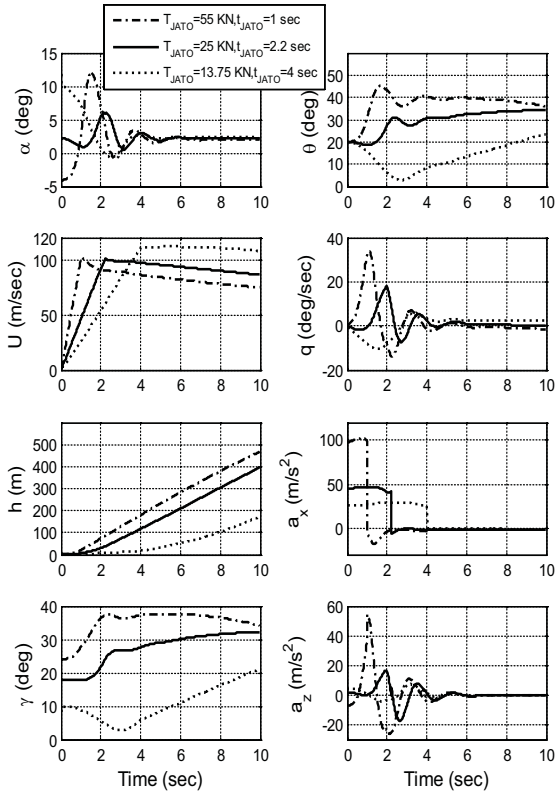

Figure 16. Case 1

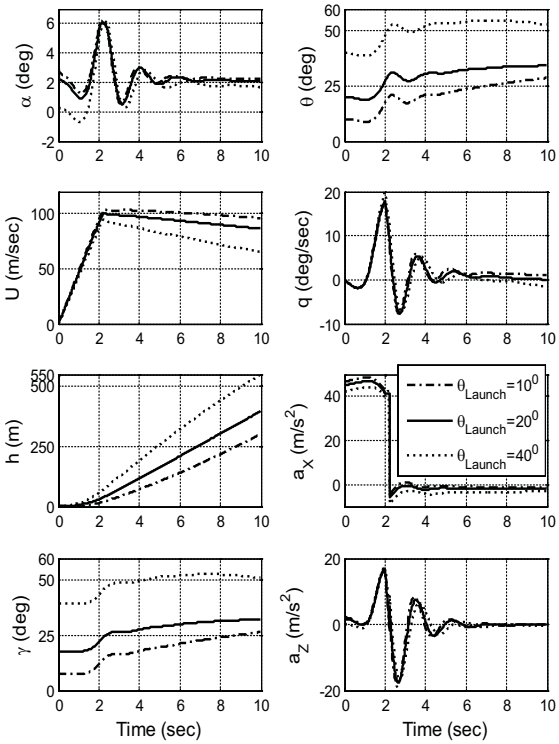

Figure 17. Case 2

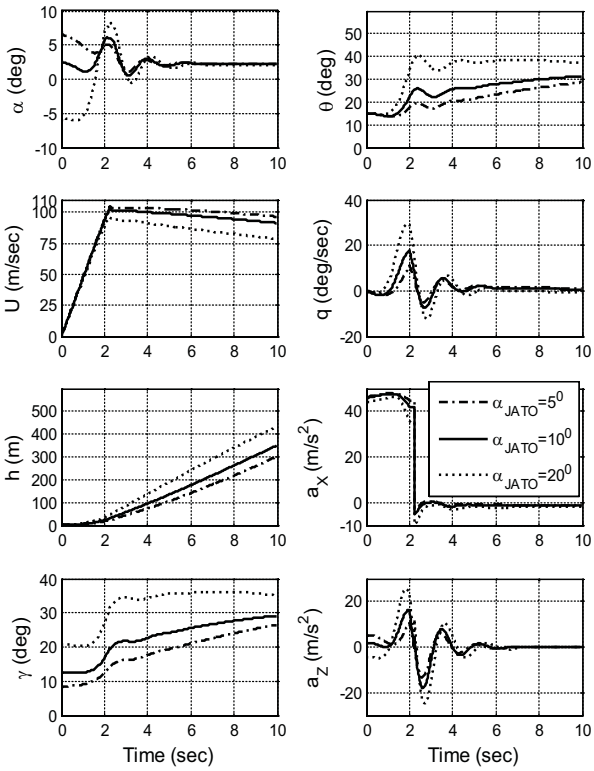

Figure 18. Case 3

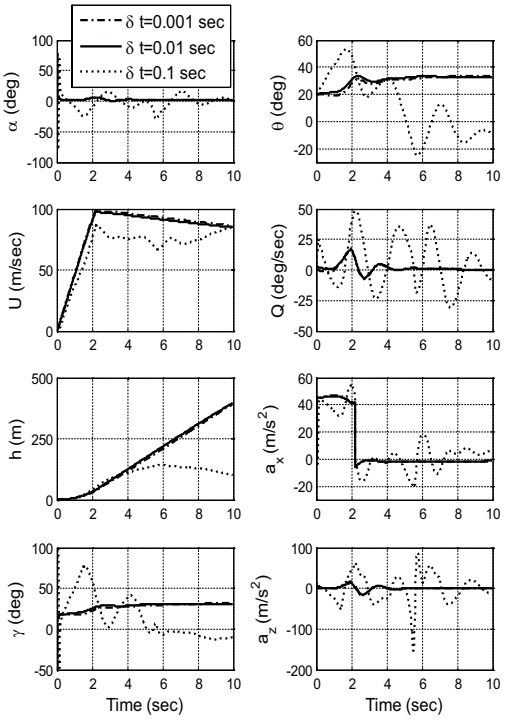

Figure 19. Case 4

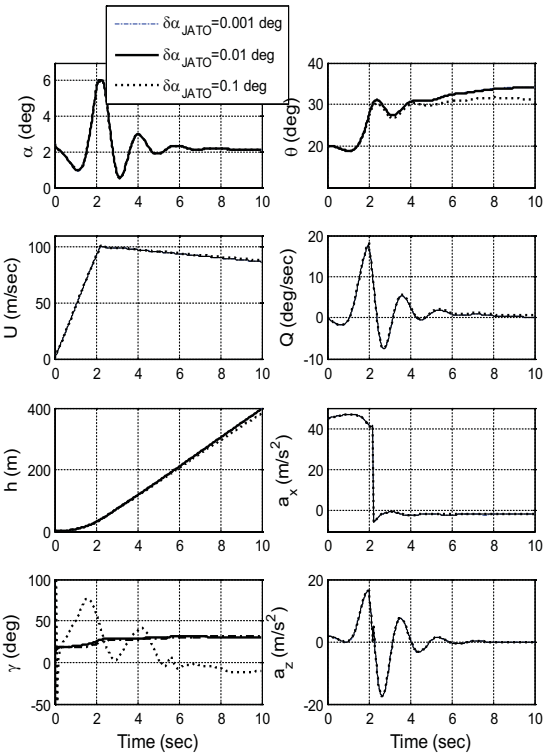

Figure 21. Case 5

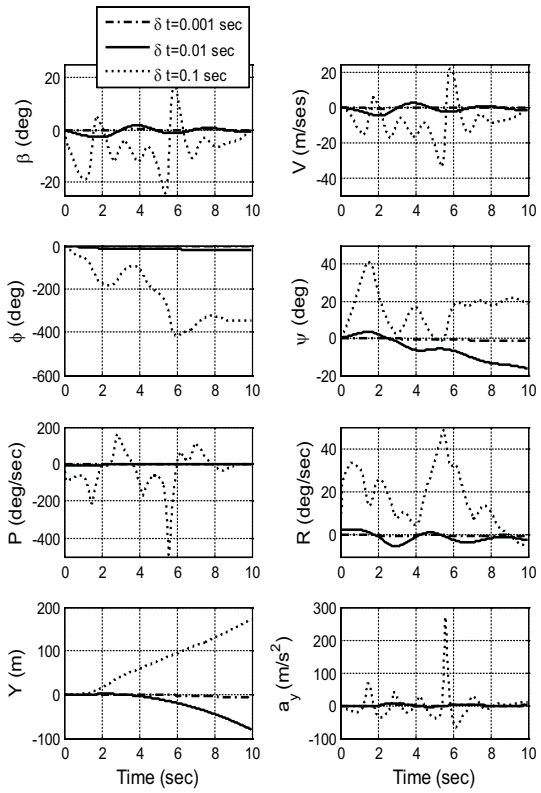

Figure 20. Case 4

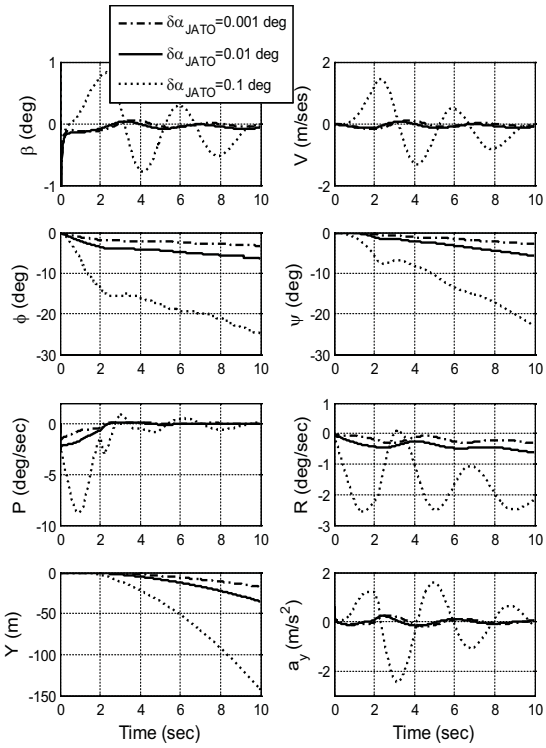

Figure 22. Case 5

Conclusions

In this paper, the simulation of UAV in the launch phase with some specific problems of this phase was developed. Accurate formulation of symmetric and asymmetric forces and moments acting on the UAV offered additional insight and understanding, which could not have been gained without simulation. Three case studies were modest examples of this simulation. Comparison of simulation and test in asymmetric condition, in conjunction with headwind and the UAV with and without engine showed an acceptable agreement between simulation and test results and a high fidelity simulation was verified. It was also important to note how the UAV would behave in these conditions and how to decide whether it is safe to launch the UAV.

The key in solving this problem was to recognize the contribution of aerodynamic forces and moments, JATO forces and moments in symmetric and asymmetric conditions, cg traveling during launch and moment coefficient variations because of cg traveling.

Sensitivity analysis was shown as a useful tool to design launch parameters. It increased the insight of the launch performance as a result of effective parameters in the launch phase. For developing the research, some measures can be done such as extending and implementing a higher fidelity simulation and using an optimization algorithm to design the launch parameters which are quantitatively more precise.

Acknowledge

The authors hereby express their gratitude for the grant support from the HESA design bureau.

References

1. Johnson, Eric N., Fontaine, Sebastiene, “Use of Flight Simulation to Complement Flight Testing of Low-Cost UAVs”, AIAA 2001-4059, 2001.
2. Brian L. Stevens & Frank L. Lewis, Aircraft Control and Simulation, John Willey & Sons INC, (1992).
3. Roskam, Jan, Airplane Flight Dynamics and Automatic Flight Controls, Jan Roskam, Kansas, (1997).
4. Louise V. Schmidt, “Introduction to Aircraft Flight Dynamis”, AIAA, 1998.
5. Cooke, Joseph M., Zyda, Michael J., Pratt, David R., McGhee, Robert B., NPSNET: “Flight Simulation Dynamic Modeling Using Quaternion”, In Presence, Vol. 1, No. 4, pp. 404-420, 1994.
6. Ralston, John, Kay, Jacob, “The Utilization of High Fidelity Simulation in the Support of High Angle of Attack Flight Testing”, Hampton, VA 23666 USA.
7. Mortazavi, Mahdi, Askari, Abdorreza, “Simulation of RPV’s launch phase”, The forth biennial conference of the Iranian aerospace society Conference, Amirkabir University of Technology, 2003.
8. Vaziri M.A., Mortazavi M., Seyyed-agha AR., Shakoori A., Askari Abdorreza, “Novel Configuration for a Civil Medium Altitude Jet Powered Unmanned Air Vehicle”, The Fourth Iranian Aerospace Society Conference, Amirkabir University of Technology, 2003.